United Nations Educational, Scientific and Cultural Organization
Geothermal Training Programme Under the auspices of UNESCO

GRÓ GTP, Urðarhvarf 8,
IS-203 Kópavogur, Iceland

Reports 2022
Number 10

GEOCHEMISTRY OF NON-THERMAL AND GEOTHERMAL WATERS, COSIGÜINA AREA, NICARAGUA

Carlos Fernando Blanco Cruz
Ministry of Energy and Mines
East side of Las Palmas Park, Managua
NICARAGUA
cacr@grogtp.is

ABSTRACT

Potential geothermal activity in the Cosigüina area, Nicaragua, was assessed based on the geochemical composition of surface and shallow groundwater in the area. Most of the waters are categorized as bicarbonate and sulphate type whereas some are chloride type. By applying multiple mineral equilibrium, Na-K-Mg ternary and silica-enthalpy geothermometry, it is concluded that most of the waters are immature and dominated by cold or non-thermal water source. Out of 25 waters samples studied, only one shows a significant geothermal water input, sample 2011 069. The calculated temperatures of a potential deep geothermal reservoir end-member fluid are uncertain and range from ~100 to ~200°C. Further studies would benefit from additional sampling in the area targeting potential geothermal waters as well as deeper boreholes that are presumably less affected by shallow non-thermal ground- and surface waters.

1. INTRODUCTION

Nicaragua, a country located in Central America, presents a significant geothermal potential due to the presence of the Maribios volcanic mountain range along the Pacific region coast. Geothermal research began in Nicaragua in the mid 1960's with the main exploration activity centred in the western part of the country (Solorzano, 1990). Today, two geothermal fields are utilized for electricity power production, the Momotombo geothermal field and the San Jacinto Tizate geothermal field (Aráuz, 2011), with a total installed capacity of 154.5 MW_e (MEM, 2022).

Among the first steps in geothermal development is geochemical exploration that uses various geochemical approaches to study geothermal water and steam that may be used to develop a conceptual model of a geothermal system. This includes, geothermometry that uses the chemical and isotopic composition of geothermal waters and gases collected at the surface to estimate subsurface fluid temperatures. Moreover, the chemical and isotope composition of geothermal waters can be used to trace the origin of the waters and mixing with cold or non-thermal waters in the upflow zone. Moreover, soil gas methods are utilized to identify fluid pathways to the surface through the distribution of geothermal gases in soil (Nicholson, 1993).

Among potential geothermal fields that has not yet been properly examined is the area around the Cosigüina volcano in northwest Nicaragua. Samples of surface waters, geothermal fluids, and non-

thermal waters were collected approximately 10 years ago, but they have not been used in further studies. In this report, these water samples from the Cosigüina area were analyzed, the different water types classified, and subsurface temperatures as well as the mixing between geothermal and non-thermal waters were assessed using geothermometry and mixing models.

2. BACKGROUND

2.1 Study area

The Cosigüina area is located at the northern end of Nicaragua's volcanic mountain range. It is situated on a peninsula formed primarily by the Cosigüina volcano and its surrounding lowlands. The Pacific Ocean is to the southwest, west, and northwest, while the Gulf of Fonseca is located to the north and northeast of the peninsula. The topography in the area is relatively soft. Elevations range from sea level to 872 meters at the highest point of the Cosigüina volcano along the peninsula. The commune population living in the area is mainly devoted to agriculture and animal husbandry as economic activities (CNE, 2001). A location map of the area is shown in Figure 1.

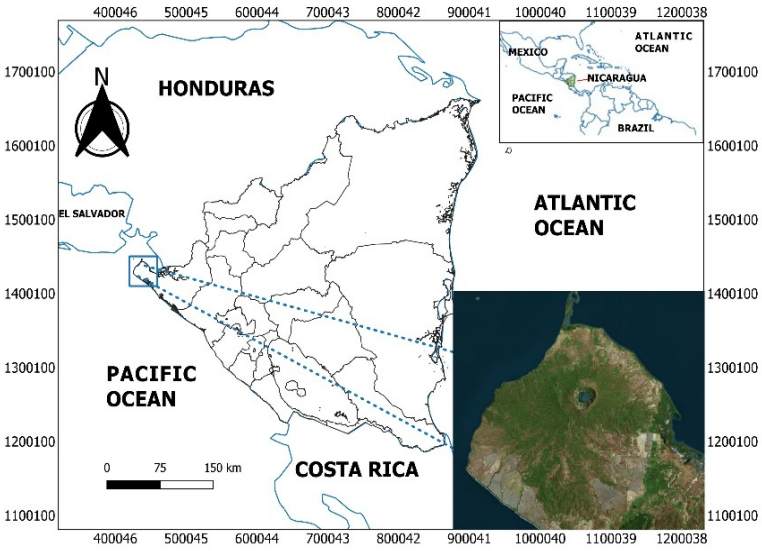

FIGURE 1: Cosigüina study area location map (blue box)

2.2 Local geology

Cosigüina volcano is a broad volcanic shield lying on the westernmost limits of the Nicaragua territory (Weyl, 1980), being part of the volcanic belt genetically associated with subduction of the Cocos plate beneath the Caribbean plate (Mann, 1995). The present-day volcano sits on the remains of an old basaltic andesite stratovolcano, probably of Pleistocene age. The basement of the Cosigüina Peninsula consists primarily of deeply weathered, fused ignimbrite and lava rocks of the Coyol Formation (Hradecký and Rapprich, 2008).

In Figure 2 we can see a generalized geological map of the Cosigüina volcano. The region has numerous small faults and lineaments to the west and east of the central volcano, most of which trend roughly in a north-south direction. They are localized and no regional extension structure has been identified (CNE, 2001). Regarding the lithology of the area, basalts, ash and sand deposits, pyroclastic flows, among others, have been identified.

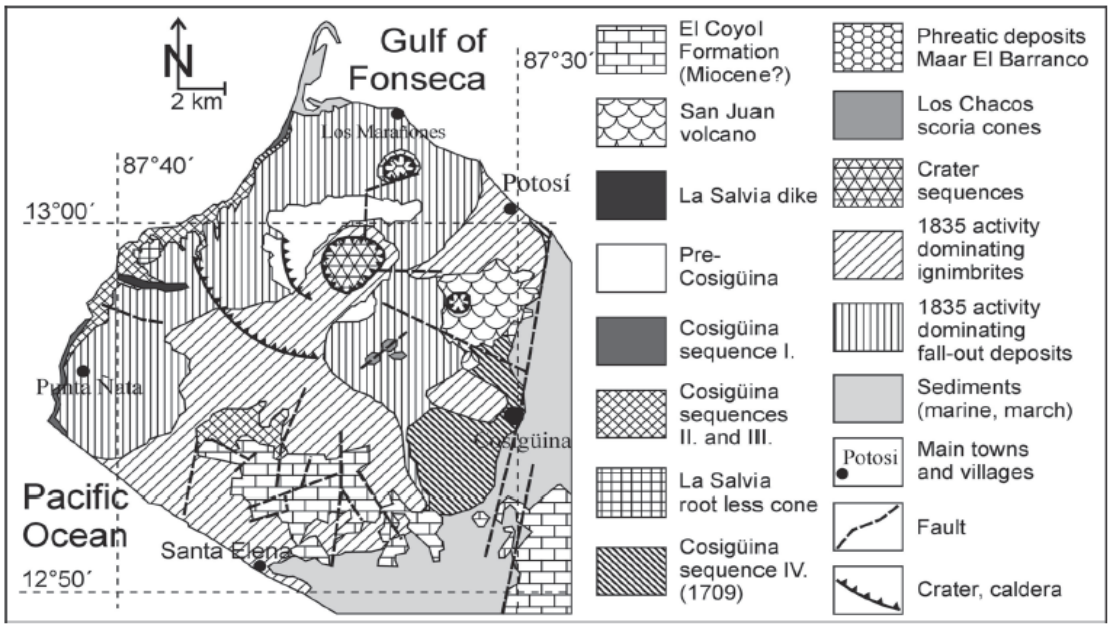

FIGURE 2: Generalized geological map of the Cosigüina Volcano
(Simplified after Hradecký et al., 2001)

2.3 Geothermal activity

In the Cosigüina peninsula some but not widespread thermal manifestations have been reported. The main natural thermal manifestations are found on the eastern shore of the peninsula whereas waters with variable temperatures between 35°C and 40°C are found. Inside the Cosigüina volcano, large areas affected by hydrothermal alteration have been observed, mainly on its S and NE wall, but without fumarolic activity. In some limited areas around the peninsula there are shallow wells with slightly anomalous temperatures and chemical compositions (CNE, 2001). Studies by Krasny and Hetch (1998) reported a water sample from the Cosigüina volcano crater lagoon collected in 1973, which indicates Na-Cl (sodium- chloride) type of water with 1890 mg/L of Cl. This suggests that the lagoon is potentially fed by some geothermal fluids from below.

3. METHODS

3.1 Sampling and analysis

Water sample collection in the Cosigüina area was carried out in 2011 by the personnel of the geochemical laboratory of the Ministry of Energy and Mines. The locations of the sampled sites are shown in Figure 3. Samples were collected from dug wells, boreholes, and springs. A total of 35 water samples were collected, 25 of which were selected for this report. On-site, pH, temperature, and electrical conductivity were analysed using a Hach HQ40d multiparametric Probe calibrated prior to sampling. Further samples were collected for laboratory analysis. These were filtered through a 0.45 µm cellulose nitrate membrane filter. Samples for cation determination were acidified using 1 ml of HNO_3 whereas samples for anion determination were not further treated. Cations, Na, K, Ca, Mg, Fe, Li, and Rb, were analysed using atomic absorption spectrophotometry with flame technique, HCO_3^- was analysed by acid-base titration, Cl by argentometric titration, B by UV-VIS spectrophotometry using the Azomethine-H method, SiO_2 by UV-VIS spectrophotometry and the molybdenum blue method, and SO_4 either by an indirect spectrophotometric method with barium chromate or bromophenol blue. Data quality was checked against charge ion balance error.

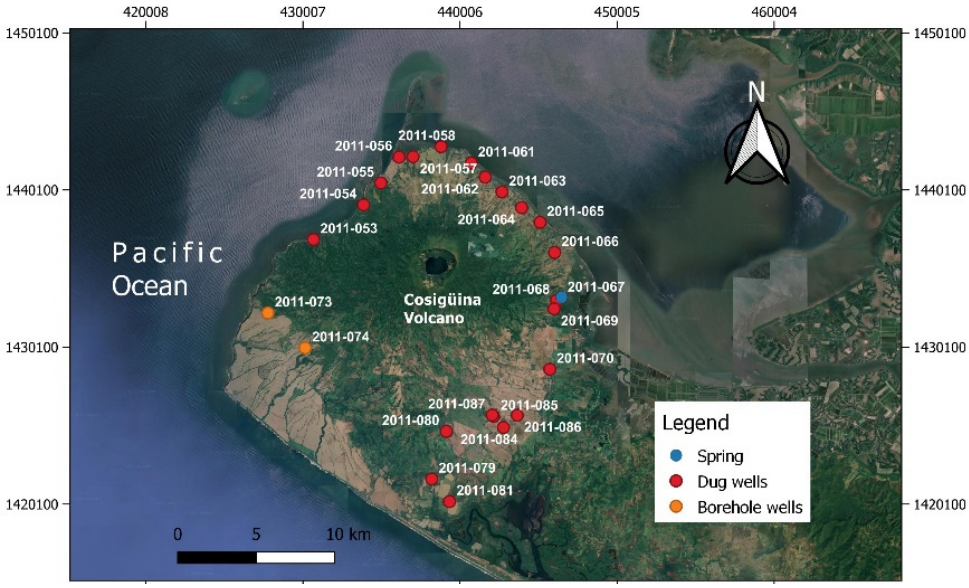

FIGURE 3: Cosigüina water samples location map

Ion balance is defined as the sum of determined anions matches the sum of determined cations Ármannsson et al., 2022),

$$CBE(\%) = \frac{\sum z_{cat} m_{cat} - \sum z_{an} m_{an}}{\sum z_{cat} m_{cat} + \sum z_{an} m_{an}} * 100\% \quad (1)$$

where z_i is the charge of an ion, i; and m_i is the molal concentration of i (mol/kg).

3.2 Classification of geothermal fluids

Ellis and Mahon (1977) classified geothermal waters based in the distribution of the concentration of major anions in the following manner:

a) Alkali-chloride water, with pH from 4 to 11, mostly sodium-potassium chloride waters.
b) Acid-sulphate water, resulting from the oxidation of H_2S forming SO_4, most constituents likely dissolved from surface rock. This kind of water is not useful for subsurface properties estimation.
c) Acid-sulphate-chloride water is a mixture of alkali-chloride water with sulphate water, it can be formed from the oxidation of H_2S to SO_4 in alkali-chloride or sulphur rock dissolution followed by oxidation.
d) Bicarbonate water might derive from CO_2 gas during the steam condensing or be the result of water mixing. It is rather common in old geothermal systems and the surrounding outflow areas, most commonly at equilibrium and useful for estimation of subsurface properties.

Various geochemical techniques may, for example, the application of geothermometry, only apply if the water is classified as mature, i.e., its chemical composition suggests that it is in equilibrium with the relevant minerals but not very much affected by mixing with non-thermal waters or re-equilibrated at surface

According to the geothermal water classification of Ellis and Mahon (1977), the data is expressed as a percentile point with a relation between the three constituents and is obtained by summing the concentration of each component in ppm:

$$S = m_{Cl} + m_{SO_4} + m_{HCO_3} \quad (2)$$

where S is the sum of all the concentrations; and c is the concentration of the anion in ppm. Therefore, the percentage of each anion is calculated as:

$$\%Cl = {}^{m_{Cl}}/_{S} \cdot 100 \quad (3)$$

$$\%SO_4 = {}^{m_{SO_4}}/_{S} \cdot 100 \quad (4)$$

$$\%HCO_3 = {}^{m_{HCO_3}}/_{S} \cdot 100 \quad (5)$$

3.3 Geothermometry

Geothermometry refers to the use of chemical composition of geothermal fluids to estimate the subsurface reservoir fluid temperature. There are different geothermometry techniques used, among others solute, gas, isotope, and multiple equilibrium geothermometry. Solute geothermometers are based on temperature dependent mineral-fluid equilibria and includes, for example, SiO_2, Na/K, Na-K-Ca, and Na-K-Mg geothermometers (Fournier and Potter, 1979; Marini et al., 1986; Nicholson, 1993).

In this study, the multiple equilibrium geothermometry technique were applied to constrain the reservoir temperatures for the most mature samples in the Cosigüina area. In this approach the saturation indices of different minerals are studied simultaneously as a function of temperature and to find the mineral suites and temperature conditions that are likely to equilibrate with the waters (Reed and Spycher, 1984).

The saturation index (SI) of the various minerals of interest was calculated by using aqueous speciation to calculate the respective reaction quotient (Q) that was compared with the equilibrium constant (K), i.e.,

$$SI = logQ - logK \quad (6)$$

when SI < 0 the solution is undersaturated with respect to the mineral and the mineral may dissolve, when SI > 0 the solution is supersaturated, and the mineral may form, at SI = 0 fluid-mineral equilibrium prevails. The calculations were conducted with the aid of the PHREEQC speciation program (Parkhurst and Appelo, 1999).

3.4 Mixing Model and Geothermometry

Mixing of various water types can take place when deep reservoir geothermal fluids mix with shallow non-thermal water. Such mixing is common in geothermal systems and makes the application of geothermometry difficult and invalid in many cases After fluid mixing, partial or complete chemical equilibration may occur and assuming no-such reactions, the initial equilibrated geothermal fluid composition is not preserved.

The two mostly applied mixing and geothermometry models in geothermal sciences are the silica-enthalpy model (Fournier, 1977) and the Na-K-Mg ternary diagram (Giggenbach, 1991). The silica enthalpy model is based on conservation of energy (enthalpy) upon mixing between a cold water and an equilibrated deep geothermal reservoir fluid in equilibrium with quartz or chalcedony. It follows that a linear trend in SiO_2 concentration with enthalpy is observed on a diagram of SiO_2 vs enthalpy that can be used to extrapolate to the silica equilibrium concentrations and hence estimate the end-member reservoir geothermal fluid temperature. Upon cooling, the fluids may, however, become supersaturated with amorphous silica that readily precipitates out of neutral to alkaline pH waters, thereby decreasing the original SiO_2 concentration of the fluids.

The Na-K-Mg ternary diagram assumes that the Na-K-Mg mineral-fluid equilibria is applicable for the deep reservoir geothermal fluids followed by mixing with non-thermal waters without any secondary reactions potentially modifying the fluid composition (Giggenbach, 1991). In order to observe the trends and potential reservoir fluid temperatures, the data are plotted on the ternary diagram after conversion

(scaling) using the following formulas:

$$S = \frac{C_{Na}}{1000} + \frac{C_K}{100} + \sqrt{C_{Mg}} \quad (7)$$

$$Na = {C_{Na}}/{10S} \quad (8)$$

$$Mg = 100\,{\sqrt{Mg}}/{S} \quad (9)$$

where S is the sum all the scaled concentrations and Ci is concentration of the cation in ppm.

4. RESULTS

In total 25 water samples were used in this report. Table 1 shows the chemical compositions of the water samples. The group of 25 water samples were taken between April and May of 2011 and analysed in the geochemical laboratory of Ministry of Energy Mines of Nicaragua. The set of samples are made up of 22 samples from dug wells, two samples from borehole wells and one sample from a spring collected in the Cosigüina area in Nicaragua.

The quality control was made by checking the ion mass balance of the samples. Figure 4 shows the charge balance error of the samples studied in this report. Most of the samples have 5% or less error between the ions, while seven samples are located between 5% and 10%. However, it is noted that a positive systematic error is observed for many samples, lying between 0 and +7%.

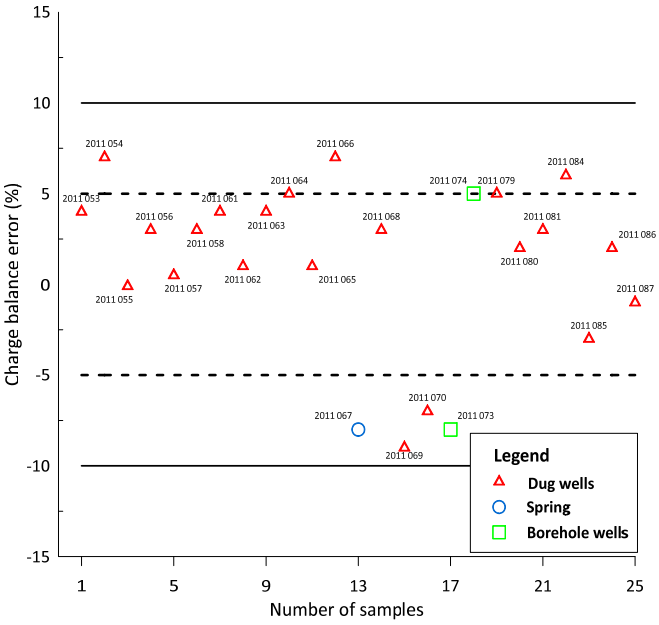

FIGURE 4: Charge balance error for Cosigüina waters, Nicaragua

The temperatures of the sampled waters ranged from 27.5°C to 42.3°C, and the pH of the water samples were close to neutral in all cases, between 6.4 and 7.6. The concentration of dissolved elements ranged over an order of magnitude with total dissolved solids (TDS) ranging from 113 to 1321 ppm.

The most important anions were HCO_3 (56-383 ppm) and SO_4 (7.1-1273 ppm), followed by Cl (4.7-655 ppm), whereas the most important cations were Ca (9.7-504 ppm), followed by Na (14.2-306 ppm), and Mg (2.5-77 ppm). Dissolved SiO_2 (57.1-106 ppm) was also an important dissolved element in the waters. The concentrations of elements (Cl, Mg, Na, and SiO_2) were observed to show increase with increasing temperature (Figure 5).

TABLE 1: Chemical composition of water samples

Sample	pH	T (ºC)	Na (ppm)	K (ppm)	Ca (ppm)	Mg (ppm)	Cl (ppm)	SO_4 (ppm)	HCO_3 (ppm)	CO_2 Total (ppm)	SiO_2 (ppm)	B (ppm)	Li (ppm)	Al (ppm)	Rb (ppm)	Fe (ppm)	TDS (ppm)
2011 053	7.6	27.5	32.2	11.8	116	70.9	61.5	208.9	383	276.3	57.1	0.009	0.01	0.027	0.028	<0.016	550
2011 054	7.3	31.1	42	10.9	90.8	15.7	29.9	133.7	197.5	142.4	90.9	0.36	0.006	0.09	0.028	0.051	332
2011 055	7.0	37.0	170.7	29.8	260.5	55.4	349.9	489	350.9	253.1	77.3	2.68	0.02	0.029	0.028	<0.016	1280
2011 056	6.9	30.7	29.2	8.8	69.8	14.9	10.4	141.7	160.8	115.9	86	0.09	<0.022	0.016	0.028	<0.016	267
2011 057	7.1	28.7	41.5	6.7	124.5	9.7	38.3	171.2	260.2	187.7	88.8	0.1	<0.022	0.054	0.028	<0.016	341
2011 058	7.0	28.5	29.1	17.2	142.8	17.9	110.5	152.6	206.8	149.2	86.5	0.09	0.004	0.12	0.028	0.02	540
2011 061	7.3	31.1	54.8	13	109.6	30.5	44.8	259.2	201.5	145.3	69.1	0.23	0.012	0.068	0.028	0.045	457
2011 062	6.9	30.9	75.8	35.8	432.4	75.3	115	1241	134.8	97.2	72.3	0.32	0.009	0.046	0.028	<0.016	1321
2011 063	6.6	31.1	37.43	10	504.3	30.7	7.9	1274	56.0	40.4	81.1	0.12	0.013	0.023	0.028	0.171	1003
2011 064	7.3	32.2	40.93	30	197.9	39.9	9	569	146.8	105.9	82.2	0.13	0.004	0.05	0.028	0.058	654
2011 065	6.9	33.0	126.7	16.2	148.8	60.1	142.5	460	265.5	191.5	80.3	1.06	0.04	0.016	0.028	<0.016	835
2011 066	6.8	37.8	57.5	11.2	77.9	18.6	77.5	108.9	150.1	108.3	95.9	0.16	<0.022	0.043	0.028	<0.016	506
2011 067	7.1	42.3	191.7	17.8	67.5	33.4	314.9	229	229.5	165.5	99.7	1.56	0.089	0.015	0.028	<0.016	884
2011 068	6.9	34.6	160.7	37.6	106.8	36.6	407.4	99.7	102.7	74.1	88.2	1.08	0.039	0.077	0.028	0.027	834
2011 069	7.1	36.1	305.5	22.5	90.9	2.5	654.8	82.1	133.4	96.2	97.3	2.44	0.051	0.021	0.028	<0.016	1290
2011 070	6.9	31.6	36.0	9.7	66.5	2.6	15.8	132.7	181.4	130.8	83.4	0.24	<0.022	0.015	0.028	<0.016	297
2011 073	7.1	27.6	29.6	9.2	177.5	30.1	16.1	497.2	238.5	172	76.7	<0.05	<0.022	0.049	0.028	<0.016	571
2011 074	7.2	29.5	29.6	9.4	216.9	77.2	13.2	633	220.9	159.4	74.4	<0.03	0.011	0.029	0.028	<0.016	653
2011 079	6.9	29.8	40.6	4.3	89.3	23.6	31.5	88.4	287.6	207.5	77.3	<0.05	<0.022	0.066	0.028	<0.016	388
2011 080	6.9	28.7	14.2	2.4	9.7	6.7	4.7	7.08	84.2	60.7	105.5	<0.05	<0.022	0.149	0.028	<0.016	113
2011 081	6.8	30.2	18.2	6.2	27.2	10.1	9.5	28	126.3	91.1	76.2	<0.05	<0.022	0.028	0.028	<0.016	214
2011 084	6.8	29.6	28.0	4.8	45.3	18.8	29.9	60.3	150.8	108.8	87.1	0.07	<0.022	0.166	0.028	<0.016	398
2011 085	6.4	30.1	39.15	7.2	64.6	37.2	50.4	171.8	227.9	164.4	84.4	0.36	<0.022	0.09	0.028	0.024	581
2011 086	6.6	31.2	53.52	8.9	176.5	51.5	104.9	347.6	291.12	209.9	79.9	0.72	<0.022	0.106	0.028	<0.016	374
2011 087	6.8	30.7	38.2	6.3	74.9	31.8	23	249	161.35	116.4	86.5	0.2	<0.022	0.036	0.028	0.045	515

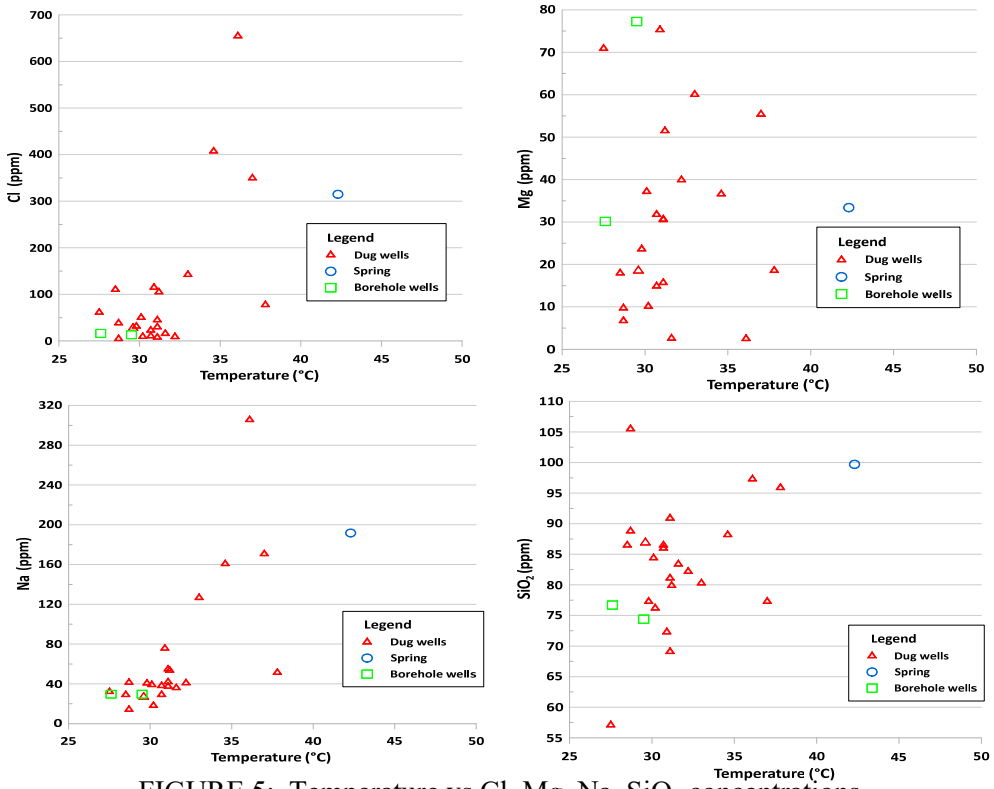

FIGURE 5: Temperature vs Cl, Mg, Na, SiO_2 concentrations measuring in Cosigüina waters, Nicaragua

5. DISCUSSION

5.1 Water classification

The classification of waters was determined using the Cl-SO_4-HCO_3 ternary diagrams, that is based on the abundance of major anions. The result is shown in Figure 6.

Most of the water samples are classified being bicarbonate (HCO_3) and sulphate (SO_4) types, which are related to peripheral waters and steam heated waters. Steam-heated waters are, however, not evident in the area these being characteristic of elevated SO_4 concentrations, low pH values, and low Cl concentrations. Three samples (2011-067–069), including the only spring sampled in the area, are classified as chloride water types.

Chloride waters may be good prospects for the use of geothermometers, however, some of these waters may be affected by other processes such as evaporation and/or mixing with non-thermal water.

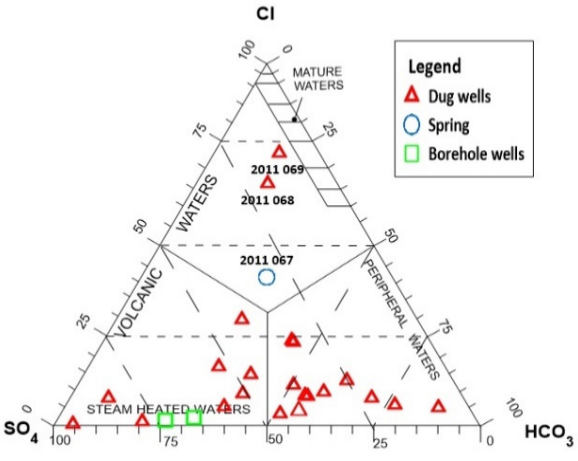

FIGURE 6: Cl-SO_4-HCO_3 diagram for Cosigüina waters, Nicaragua

5.2 Geothermometry and mixing

One sample shows the most significant signature of a geothermal water input (2011 069). The sample is from a dug well, has a high Cl concentration (655 ppm), among the lowest Mg concentration (2.5 ppm), and among the highest SiO_2 concentration (97.3 ppm). Such trends are considered an indication of geothermal water potentially mixed with non-thermal water (D'Amore and Arnórsson, 2000).

The results of the multiple mineral-water geothermometry for the sample is shown in Figure 7. According to Reed and Spycher (1984), the temperature at which the log (Q/K) curves intersect each other (SI = 0) is the equilibration temperature. They described that the characteristic convergence of SI curves for the equilibrium assemblage to zero at the temperature of equilibration establishes the basis for determining a mineral assemblage and temperature of equilibration of natural geothermal waters.

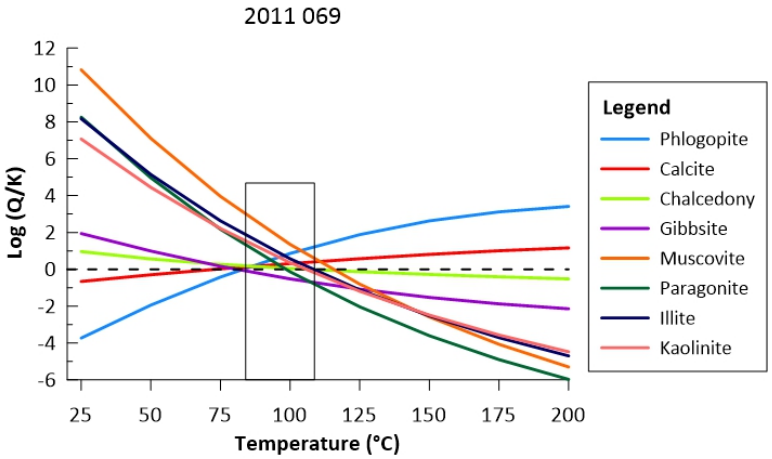

FIGURE 7: Multi mineral equilibrium plot for sample 2011 069. The rectangle represents the equilibrium temperature range of the minerals

The minerals include are those often associated with low temperature geothermal activity, for example, oxides and hydroxides (chalcedony and gibbsite), carbonates (calcite), clays (illite, kaolinite), and micas (phlogopite, muscovite, paragonite). It should be noted that common geothermal alteration minerals like feldspars, epidote, and amphibole may not be the suitable minerals to assemble in under such low temperature geothermal conditions (Browne, 1978).

Based on the results shown in Figure 7, the equilibrium geothermometry temperature for the water is ~100°C (96±13°C); the rectangle in the middle of the plot indicates the equilibrium temperature range obtained from the minerals. However, it should be noted that this conclusion does not consider the possible mixing of the geothermal water component with non-thermal water.

Many of the water samples considered in this study are presumable mixtures of cold or non-thermal water and geothermal water. Such mixing trends can be assessed using, for example, the Na-K-Mg ternary diagram (Giggenbach, 1988) and the silica-enthalpy diagram (Fournier, 1977).

As seen in Figure 8, the Na-K-Mg ternary diagram indicates that most waters are immature and have very similar chemical compositions as cold or non-thermal water. Most of the samples are close to the Mg apex. This indicates an interaction between the water and the rocks at relatively low temperatures. Only one sample has potentially some significant geothermal input, sample number 2011 069, that was used in the previous calculations by applying multiple mineral equilibria geothermometry. According to the results of the Na-K-Mg diagram, sample 2011 069 shows a signature of potential geothermal water mixing with cold or non-thermal water. Linear extrapolation assuming non-reactive behaviour upon mixing suggests geothermal reservoir temperatures as high as ~200°C compared to the results of ~100°C based on the multiple mineral equilibrium geothermometry. Moreover, it should be pointed out that the "fully equilibrium waters" curve proposed by this diagram is based on a water-mineral equilibrium involving K-feldspars, albite, mica, and chlorite (Giggenbach, 1988); whereas the multiple

mineral equilibrium geothermometry (Figure 7) is based on a selection of different alteration minerals more common at low-temperatures and includes oxides and hydroxides, various clays, carbonates, micas, and sometimes sulphides and sulphates (Browne, 1978).

Similar mixing trends may be drawn based on the evidence from the silica-enthalpy mixing model diagram in Figure 9. In the model it is assumed that conductive cooling does not occur in the up flow after mixing and that there is no change in the aqueous silica concentration. According to the results, most of the waters are non-thermal waters with SiO_2 concentration similar to the solubility of amorphous silica at the measured temperatures (Gunnarsson and Arnórsson, 2000) or the chalcedony geothermometer temperature of ~112-150°C; this depends on the assumption that only conductive cooling (orange line in Figure 9) vs. non-reactive mixing between the cold or non-thermal water and the geothermal water (green line in Figure 9). The temperatures were obtained from the steam tables using the enthalpies from the plot.

The silica-enthalpy plot and the Na-K-Mg ternary diagram both support the findings that most of the water samples studied have an insignificant geothermal water component with one exception, sample number 2011 069. Based on the Na-K-Mg and the silica-enthalpy diagrams, it is however evident that this sample is also a subject of mixing of geothermal water with cold or non-thermal water and potentially also conductive cooling and re-equilibration with minerals like amorphous silica. It is therefore very hard, based on the present dataset, to define the nature of a potential deep reservoir geothermal fluids occurring in the Cosigüina area, Nicaragua.

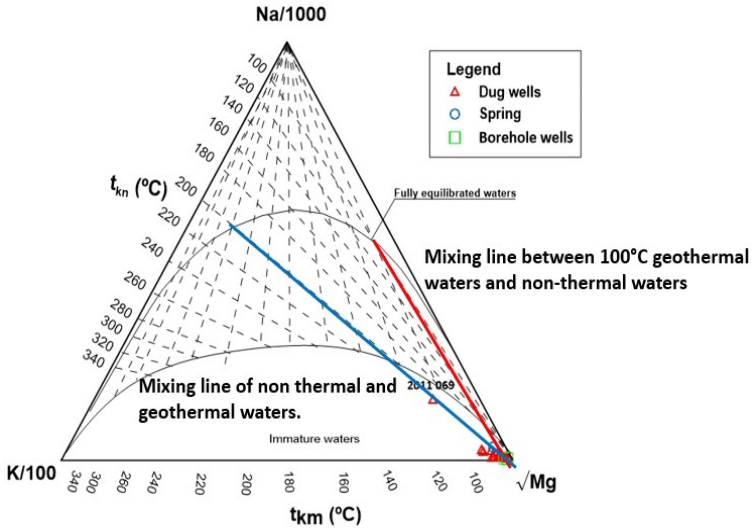

FIGURE 8: Na-K-Mg diagram for Cosigüina waters, Nicaragua

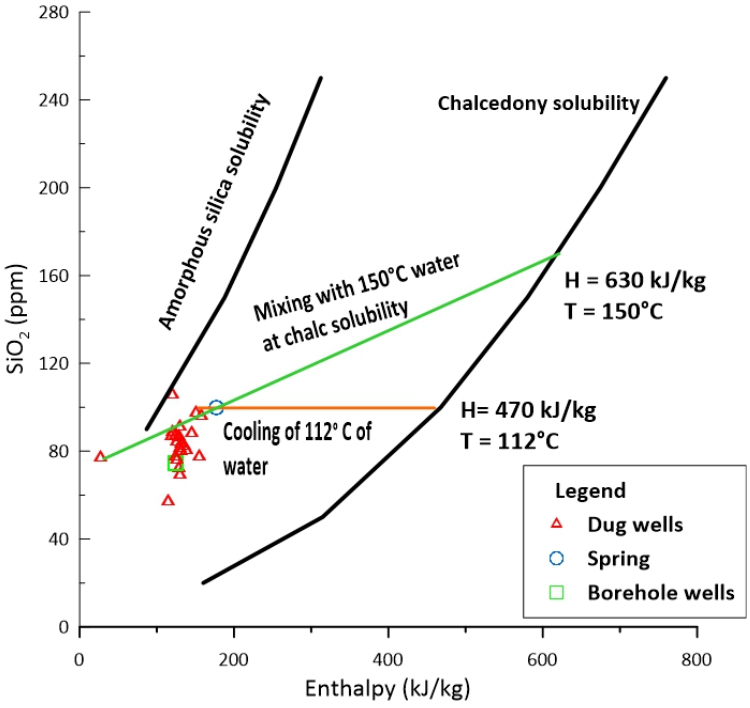

FIGURE 9: Silica enthalpy mixing model for Cosigüina waters, Nicaragua. The chalcedony and amorphous silica solubilities curves are based on data reported by Fournier (1977) and Gunnarsson and Arnórsson (2000)

5.3 Limitation of the dataset

The data of water samples collected by the Ministry of Energy and Mines and used in this study are mainly surface waters and shallow dug holes with one spring. Such waters are always potential sources of mixing and contamination of geothermal waters with non-thermal waters. Most of the samples display insignificant sign of geothermal water, i.e., have elevated Mg concentrations, low Cl concentrations, and moderate SiO_2 concentrations. One sample of the dataset indicates a significant geothermal water input and when applying classical geochemical approaches, a potential deep geothermal reservoir temperature of 100-200°C is calculated, indicating a low to medium temperature geothermal field. Water samples from deeper boreholes could potentially verify such an existence of geothermal waters but are unavailable at present.

6. CONCLUSION

In this study, the chemical compositions of 25 water samples from Cosigüina, Nicaragua, were used to assess potential geothermal activity in the area. The water samples are categorized mainly as bicarbonate and sulphate water types with some being of chloride type. Applying multiple mineral equilibrium geothermometry, the Na-K-Mg ternary diagram and the silica-enthalpy diagram, it is concluded that most of the water samples are cold or non-thermal waters with potentially one sample showing significant geothermal water input, sample number 2011 069. The calculated temperatures of a potential deep geothermal reservoir end-member fluid range from ~100 to ~200°C according to multiple mineral equilibrium geothermometry and Na-K-Mg ternary diagram. The silica enthalpy mixing model diagram calculated temperatures in a range from 112 to 150°C assuming conductive cooling and non-reactive mixing. Further studies would benefit from additional sampling in the area targeting potential geothermal waters as well as deeper boreholes that are presumably less affected by shallow non-thermal or cold ground and surface waters.

ACKNOWLEDGEMENTS

I would like to express my gratitude to Dr Guðni Axelsson and the entire GRÓ GTP team for their support and assistance throughout the training program here in Iceland. My special thanks also to the Government of Reconciliation and National Unity of Nicaragua for giving me the opportunity to participate in this program. I would like to thank to Finnbogi Óskarsson for sharing his knowledge and experience. I want to express my gratitude to my supervisor, Prof. Dr Andri Stefánsson, for his advice during the preparation of this report. And my deepest thanks go to my family for their support and encouragement during the period of the training programme.

REFERENCES

Ármannsson, H., Óskarsson, F. and Friðriksson, T. (2022): Geochemical Exploration Techniques. In *Comprehensive Renewable Energy (Second Edition)*, 80-97.

Aráuz, M.A., 2011: Environmental monitoring of geothermal projects in Nicaragua. Report 6 in: *Geothermal Training in Iceland 2011*. UNU-GTP, Iceland, 35-66.

Browne, P.R.L., 1978: Hydrothermal alteration in active geothermal fields. *Annual Reviews of Earth and Planetary Science, 6,* 229-250.

CNE, 2001: *Nicaragua geothermal master plan*. Cosiguina Volcano area evaluation, National Energy Commission of Nicaragua (CNE) and GeothermEX, Vol II, 205 pp.

D'Amore, F., and Arnórsson, S., 2000: Geothermometry. In: Arnórsson, S. (ed.) 2000: Isotopic and chemical techniques in geothermal exploration, development, and use: sampling methods, data handling, interpretation. *International Atomic Energy Agency, Vienna,* 152-199.

Ellis, A.J. and Mahon, W.A.J., 1977: *Chemistry and geothermal systems*. Academic Press, New York, 392 pp.

Fournier, R.O., 1977: Chemical geothermometers and mixing models for geothermal systems. *Geothermics, Vol 5,* 41-50.

Fournier R.O. and Potter R.W., 1979: Magnesium correction to the Na-K-Ca chemical geothermometer. *Geochim. Cosmochim. Acta, Vol 43*, 1543-1550.

Giggenbach, W.F., 1988: Geothermal solute equilibria. Derivation of Na-K-Mg-Ca geoindicators. *Geochim. Cosmochim. Acta, Vol 52*, 2749-2765.

Giggenbach, W.F., 1991: Chemical techniques in geothermal exploration. In D'Amore, F. (Ed.): *Application of Geochemistry in Geothermal Reservoir Development.* UNITAR/UNDP Centre on Small Energy Resources, Rome, 119-144.

Gunnarsson, I., and Arnórsson S., 2000: Amorphous silica solubility and the thermodynamic properties of $H_4SiO_4°$ in the range of 0° to 350°C at P_{sat}. *Geochim. Cosmochim. Acta, Vol 64*, 2295-2307.

Hradecký, P., and Rapprich, V., 2008: Historical tephra-stratigraphy of the Cosiguina volcano (Western Nicaragua). *Geological Journal of Central America, Vol 38*, 65-79.

Hradecký, P., Havlíček, P., Mayorga, E., Opletal, M., Rapprich, V., Šebesta, J. and Ševčík, J., 2001: *Geological study: Research on natural hazards and vulnerability of geological environment in the region of the Cosigüina volcano*. Archives INETER Managua and CGS, Prague [unpublished report], 36 pp.

Krasny, J., and Hecht, G., 1998: *Hydrogeologic and hydrochemical studies of the Pacific region of Nicaragua. COSUDE: INETER: GTZ*, Managua, Nicaragua, 154 pp.

Mann, P. (ed.), 1995*:* Geologic and tectonic development of the Caribbean Plate boundary in Southern Central America. *Geol. Soc. Am. Spec., Paper 295*, USA, 349 pp.

Marini, L., Chiodini, G., and Cioni, R., 1986: New geothermometers for carbonate-evaporite geothermal reservoirs. *Geothermics, Vol 15,* 77-86.

MEM (Ministry of Energy and Mines), 2022: *Interactive map of the energy and mining sector,* website: *https://energiayminas.mem.gob.ni/Generacion.aspx*

Nicholson, K., 1993*: Geothermal fluids: chemistry and exploration techniques*. Springer Verlag, Berlin, 263 pp.

Parkhurst, D.L., and Appelo, C.A.J., 1999: *User's guide to PHREEQC (version 2) – A computer program for speciation, batch-reaction, one-dimensional transport, and inverse geochemical calculations*. U.S. Geological Survey Water-Resources Investigations, Denver, Colorado, report 99-4259, 312 pp.

Reed, M.H., and Spycher, N.F., 1984: Calculation of pH and mineral equilibria in hydrothermal water with application to geothermometry and studies of boiling and dilution. *Geochim. Cosmochim*. *Acta, Vol 48,* 1479-1490.

Solorzano, M.G., 1990: Initial temperature distribution in the Momotombo geothermal field, Nicaragua, Report 6 in: *Geothermal Training in Iceland 1990*. UNU-GTP, Iceland, 01-33.

WEYL, R., 1980: *Geology of Central America*, Gebründer Borntraeger, Germany, 371 pp.